Influence of defects in a coupled map lattice modeling earthquakes

Horacio Ceva
Departamento de Física, Comisión Nacional de Energía Atómica, Avenida del Libertador 8250, 1429 Buenos Aires, Argentina

(Received 1 August 1994; revised manuscript received 28 November 1994)

We study the robustness of self-organized criticality in the coupled map lattice introduced by Olami, Feder, and Christensen [Phys. Rev. Lett. **68**, 1224 (1992)] by considering the influence of point and extended defects. Our results indicate that there is a finite range of defect concentrations for which one can observe criticality. Additionally, the study of the Gutenberg-Richter law allowed us to verify that the defect-free model has a smoother behavior than previously predicted.

PACS number(s): 05.20.−y, 05.45.+b, 05.70.Jk, 64.60.−i

I. INTRODUCTION

Self-organized criticality (SOC) was introduced as a subject of study by Bak, Tang, and Wiesenfeld [1]. It is a concept designed to describe extended dynamical systems reaching a stationary state characterized by power-law distribution functions in both space and time, without any "fine tuning" of an external parameter. Since the publication of their work there were many attempts to understand under what conditions a given system will display this behavior (see, for instance, Refs. [2, 3]).

Recently, Olami, Feder, and Christensen [4] (OFC) introduced a continuous, deterministic, nonconservative coupled map lattice model which was shown to display SOC. This model, which has had some points of contact with the work of Feder and Feder [3], can be shown to be a two-dimensional implementation of the Burridge-Knopoff spring-block model of earthquakes [5]. The model is very simple, and its properties can be controlled by means of a physically sensible parameter α measuring the degree of conservation. In fact, it was even suggested [6] that these models should be considered as generic "Ising models" of dissipative many-body systems (for a very different point of view, however, see the work of Socolar, Grinstein, and Jayaprakash [7]).

It is therefore interesting to study the different properties of this coupled map lattice. In this work we address the question of the stability of its self-organized critical solution. Also, an improved result [8] for the dependence of the Gutenberg-Richter exponent (see below) with α is given.

We chose to perturb the system by randomly introducing controlled, local variations of the coupling between nearest neighbors. We believe that this is a sensible form to introduce perturbation in a model related to earthquakes, because by breaking translation invariance we make room for inhomogeneities of the medium. More specifically, we have considered perturbed regions where earthquake strength is effectively diminished by using a smaller value of α: this seems to be the most efficient form to destroy SOC [9].

II. THE MODEL

The two-dimensional spring-block model of earthquakes consists of a set of blocks on a two-dimensional square lattice; nearest neighbor blocks are connected by springs. There is static friction between each block and the plate on which they stay, so that the force required to move a block should at least be equal to a threshold value F_{th}. As is well known, the existence of this threshold introduces nonlinearity in the problem. The last element defining the geometry of the model is a second plate, located above the blocks and connected to them by another set of springs. This gives rise to a nonconservative mechanism (a mechanism not conserving the *force* in the plane).

Moving one plate relative to the other uniformly increases the force on each block until one of them reaches F_{th}: this starts an earthquake. A block at site (i,j) and subjected to a force $F_{i,j} > F_{th}$ will move and relax by acting on its neighbors, specifically [4]

$$\begin{aligned} F_{i\pm1,j} &\to F_{i\pm1,j} + \delta F_{i\pm1,j}\ , \\ F_{i,j\pm1} &\to F_{i,j\pm1} + \delta F_{i,j\pm1}\ , \\ F_{i,j} &= 0, \end{aligned} \tag{2.1}$$

where

$$\begin{aligned} \delta F_{i\pm1,j} &= \alpha F_{i,j}, \\ \delta F_{i,j\pm1} &= \alpha F_{i,j}. \end{aligned} \tag{2.2}$$

By writing the equations in this form [i.e., the same value of α in both lines of Eq. (2.2)] we are limiting ourselves to the isotropic case.

If $\alpha = 0.25$ the system is conservative, in the sense that $\sum_{\langle \mathrm{NN}\rangle} \delta F_{\langle \mathrm{NN}\rangle} = F_{i,j}$. Otherwise, for $\alpha < 0.25$, it is nonconservative. The main properties of the model depend on the degree of conservation, i.e., on the value of α.

We have studied the case of *open* boundary conditions; this means that the outer blocks of the model are coupled to fictitious blocks with springs characterized by the same value of α. The coupled map lattice of OFC mimics this model through the following rules: a real variable $u_{i,j}$ (the "stress") is defined on each site of an $L \times L$ square lattice, with random initial values. The system is globally driven: all $u_{i,j}$ are increased simultaneously at a uniform rate, until eventually one site reaches a threshold value u_{th} ($u_{th} = 4$ in this work), triggering an avalanche. During the avalanche, the stress values of the lattice are updated as follows: for any site with $u_{i,j} > u_{th}$, $u_{i,j} \to 0$ (it topples); any site having a toppling site as a nearest neighbor is kicked: $u_{i,j} \to u_{i,j} + \alpha \sum_{\langle nn \rangle} u_{\langle nn \rangle}$. The sum runs over all the toppling nearest neighbors of site (i, j).

III. RESULTS AND DISCUSSION

In this paper we report determinations of the (normalized) distribution of earthquake sizes $D(S)$ [10]. Real earthquakes follow the Gutenberg-Richter law [11]: the number of observed earthquakes with energy ϵ greater than E is given by $N(\epsilon > E) \sim E^{-B}$, with $B = 0.80 - 1.54$. It can be shown [8] that one can write $D(S) \sim S^{-(1+B)}$ with the value of B controlled by α. The dependence of the exponent B on α found by Christensen and Olami displays an apparent change of behavior around $\alpha \sim 0.10 - 0.15$ (we reproduce data points from Fig. 3 of Ref. [8] in our Fig. 1). We have made a more detailed determination of $B(\alpha)$ for the same 35×35 lattice. It can be seen in Fig. 1 that our results are coincident with those of Ref. [8] for $\alpha \geq 0.15$, but depart from them for $\alpha \leq 0.10$.

All results quoted in this work were obtained by considering 500 independent samples. The initial configuration of each sample was chosen by randomly assigning a value to the stress at each site, such that $u_{i,j} \leq u_{th}$. For every sample we discarded the first N_r earthquakes and collected data for the following N_a. For $\alpha \geq 0.13$ we used $N_r = 5 \times 10^4$ and $N_a = 10^4$, but for $\alpha \leq 0.12$ we were forced to use $N_r = 5 \times 10^5$ to have stable solutions (i.e., we discarded 250 000 000 avalanches for these values of α). As a further check that the system is already in the stationary regime, we made extensive determinations for $\alpha \leq 0.1$ in a *single* sample, with $N_r = 1$ to 3×10^8,

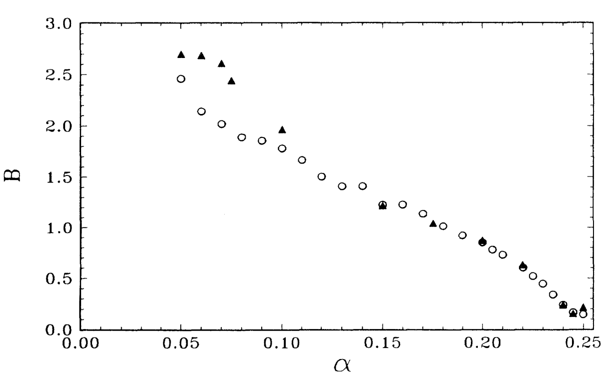

FIG. 1. The Gutenberg-Richter coefficient B as a function of α. The filled triangles represent data from the work of Christensen and Olami (Ref. [8]).

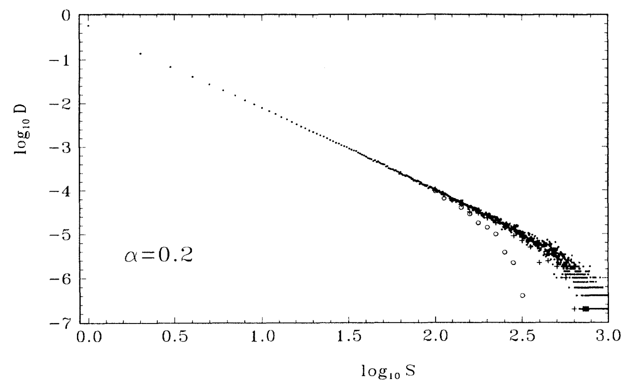

FIG. 2. Distribution function $D(S)$ as a function of S of lattices without defects and $L = 25, 35$, and 45. For $S < 100$ we only plot data for $L = 45$ (small filled triangles) because the three cases are almost indistinguishable. For $S > 100$ we have included *a few* representative, equally spaced points for $L = 25$ (empty circles) and $L = 35$ (pluses).

and $N_a = 10^5$, obtaining results in agreement with Fig. 1. The difference between these results and the work of Christensen and Olami is most probably due to this factor. Hence, our result shows that B is a rather smooth function of α, with no significant change of behavior.

The main results of this work are related to the in-

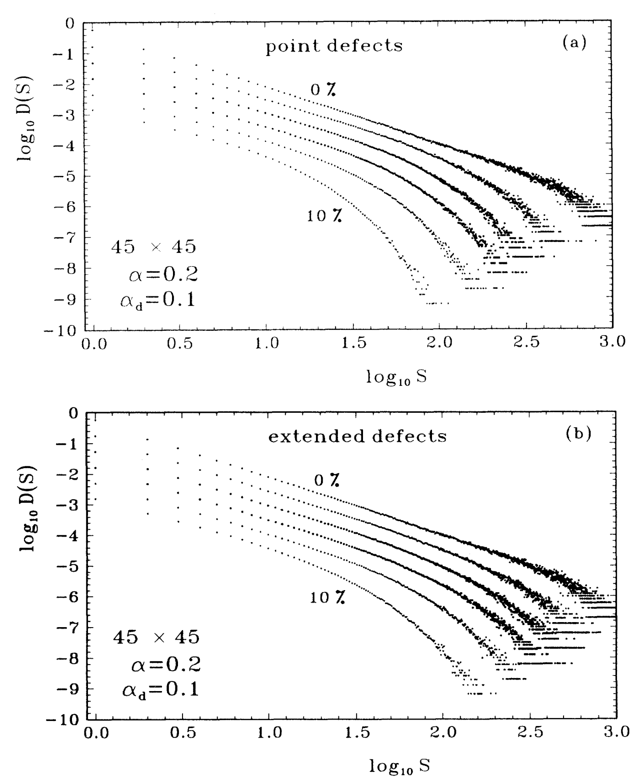

FIG. 3. Distribution function $D(S)$ of a 45×45 lattice with defects. From top to bottom, the curves correspond to 0%, 1%, 2%, 3%, 5%, and 10% of defects (all but the first curves are offset vertically 0.5 units from the previous one to improve readability).

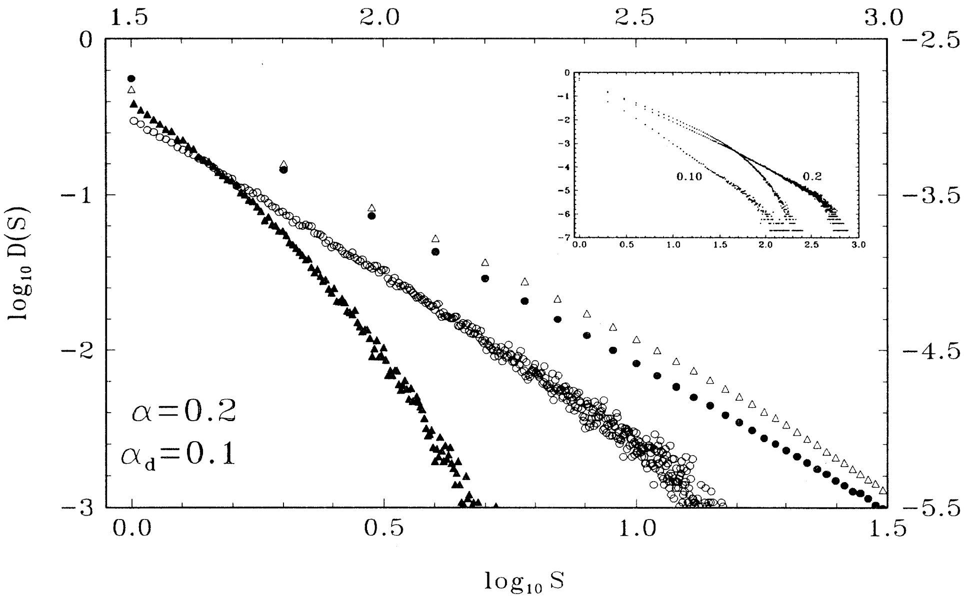

FIG. 4. Distribution function $D(S)$ for the 35×35 lattice. The curves are folded: filled circles and empty triangles correspond to 0% and 3% of point defects, respectively (left and bottom axes), while empty circles and filled triangles represent the same curves but with the upper and right axes. In the inset we show how the 3% curve interpolates between the defect-free cases with $\alpha = 0.1$ and $\alpha = 0.2$.

fluence of lattice defects. Translation invariance requires that α be the same at every lattice site. The system was perturbed by the introduction of defects: we say that a site has a (point) defect if the interactions with its nearest neighbors are changed: $\alpha \to \alpha_d$.

We have considered the influence of two different types of perturbations: point and extended defects (an extended defect is a set of contiguous point defects). Point defects were randomly assigned to different sites in the lattice.

In the other case, both horizontal and vertical straight extended defects were randomly located on the lattice with the only (arbitrary) limitation that their length be not greater than 1/10 of the lattice side. In this form we excluded cases with just one big linear defect that could eventually split the lattice in two regions.

In both cases we controlled the total number of sites with a defect, N_d. For every lattice size we used a number of sites with defects such that they represented 1%, 2%, 3%, 5%, 7%, and 10% of the total.

We have performed numerical simulations on square lattices of different sizes. Finite-size effects were taken into account by studying lattices with $L = 25, 35$, and 45. As mentioned before, all results quoted here were obtained by considering 500 independent samples, with $\alpha = 0.2$ and $\alpha_d = 0.1$.

In general, we used $N_r = 5 \times 10^4$ and $N_a = 10^4$. In several cases we also used $N_r = 1.1 \times 10^5$ to check the stability of our results. In a few cases we made runs with $N_r = 10^6, N_a = 5 \times 10^4$.

Our results for samples without any defect reproduce those of [8], as expected. Values for all three lattices coincide for $S < 100$, and show the same typical noisy behavior at the highest S values. Figure 2 displays our data for $L = 45$ and a few representative points with $S > 100$ for $L = 25$ and 35, to exhibit the L dependence as clearly as possible. It can be seen that there is no significant size effect, except for the obvious size dependence at the highest values of S.

The presence of defects changes this behavior. If the amount of defects δ exceeds $\approx 5\%$ of the sites it is no longer possible to identify a power law in $D(S)$: the system ceases to display SOC. For smaller values of δ the model apparently still has SOC, although the corresponding range of S values shrinks as δ grows, as shown in Fig. 3, were we have displaced the curves for clarity.

A closer look, however, reveals a more complex situation in the SOC region. Figure 4 shows our results for a typical case (note that the curves are folded). The sample with defects roughly interpolates between the defect-free samples with parameters α and α_d (see the inset of Fig. 4) For large values of S ($S \simeq 100$ or more) there are fewer earthquakes in the sample with defects, as expected, because $N \sim S^{-B}$ and $B(0.1) > B(0.2)$. On the other hand, for small values of S one could expect that this part of the curve with defects should be steeper than the curve without defects, while the opposite is obtained.

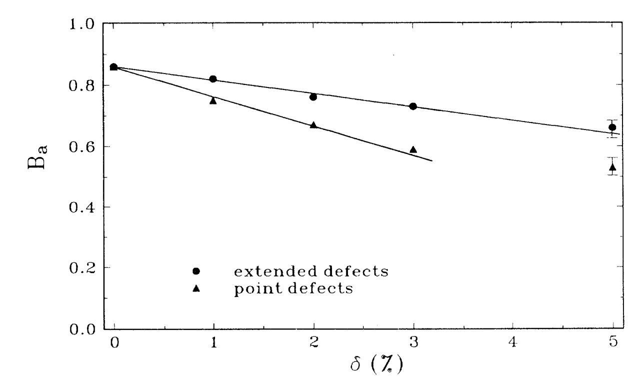

FIG. 5. Variation of the Gutenberg-Richter coefficient B_a with the defect content ($L = 45$). Data for higher values of δ do not display SOC. In the text we explain why we call this an apparent B.

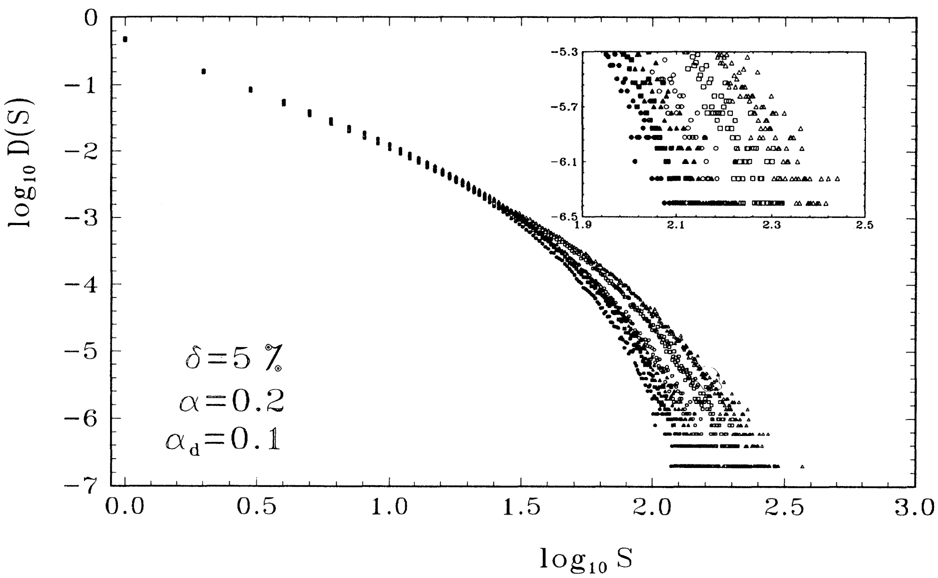

FIG. 6. Distribution function $D(S)$ for a fixed value of δ and several lattice sizes. The inset shows the noisy part in more detail. Point defects are drawn with filled symbols (circles, squares, and triangles corresponding to $L = 25, 35$, and 45, respectively); empty symbols correspond to extended defects.

In other words, it seems that it is not possible to study the influence of even a small amount of defects by isolating different regions of $D(S)$. This is probably due to the nonlocal character of the actualization rules of the cellular automaton (and to the proximity to a non-SOC state). In Fig. 5 we represent this by showing the change of B as a function of δ; we have called this $B_a(\delta)$ in order to emphasize that this can be an "apparent" B value. From both Figs. 3 and 5 it is also easy to see that point defects have a stronger effect on the model than extended defects. For $L = 25$ and 45 we found similar results.

It is instructive to consider all data corresponding to

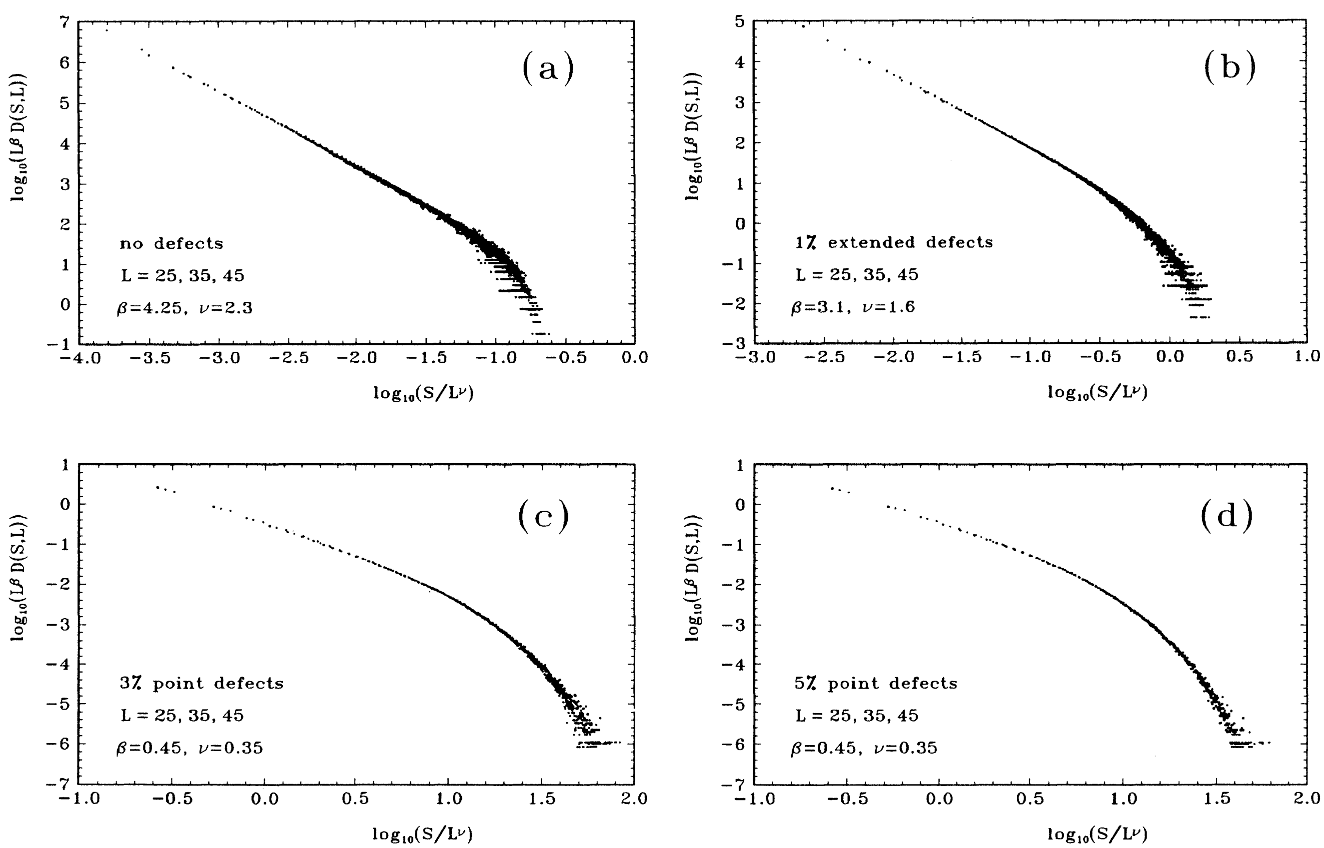

FIG. 7. Finite-size analysis for $\alpha = 0.2$ and several defect concentrations.

TABLE I. Critical exponents ν and β of the model with open boundary conditions, as a function of defect concentration. P (E) denotes point (extended) defects. B_a is the "apparent" value of B (see the text).

defects (%)	$\nu(\pm 0.1)$	$\beta(\pm 0.1)$	$\beta/\nu - 1$	B_a
0	2.30	4.25	0.85 $\pm$0.12	0.86
1 (P)	1.13	1.90	0.60 $\pm$0.23	0.75
2 (P)	0.55	0.90	0.64 $\pm$0.48	0.67
3 (P)	0.35	0.45	0.29 $\pm$0.65	0.59
5 (P)	0.35	0.45	0.29 $\pm$0.65	0.53
1 (E)	1.60	3.10	0.94 $\pm$0.18	0.82
2 (E)	1.00	1.80	0.80 $\pm$0.28	0.76
3 (E)	0.60	1.10	0.83 $\pm$0.31	0.73
5 (E)	0.60	1.00	0.83 $\pm$0.31	0.66

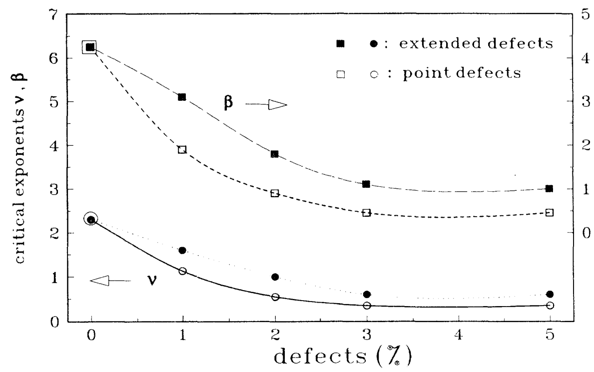

FIG. 8. Critical exponents β and ν as a function of defect concentration. The lines are only a guide to the eye.

a given percentage of defects, for instance $L = 25, 35, 45$ and $\delta = 5\%$ for both types of defects (see Fig. 6). Defects have little effect on the smallest "avalanches": this gives rise to the short straight part of the graph, for $S \leq 10$, which is analogous to the case $\delta = 0$. For larger values of S, the curves bend and spread: we show in the inset of Fig. 6 that the "order" of these curves is $25P, 35P, 45P, 25E, 35E, 45E$ ($25P$ means $L = 25$, point defects, etc.). The spread is less pronounced for smaller values of δ.

We have performed a finite-size scaling analysis of the distribution function, finding that it is very well described by the standard expression

$$D(S, L) = L^{-\beta}\mathcal{D}(S/L^{\nu}), \tag{3.1}$$

where $\mathcal{D}$ is a scaling function and β and ν are critical indices of the distribution. In other words, this result shows that the model has true criticality (for a different conclusion in a related work see Ref. [12]). We study the case $\alpha = 0.2$ as a function of both size and defect concentration. Some representative examples are given in Fig. 7. Our results are given in Table I and are displayed in Fig. 8. In Table I we also include a column with the value $(\beta/\nu - 1)$, which should be compared with B (scaling predicting [8] that $1 + B = \beta/\nu$).

In conclusion, we have shown that self-organized criticality in the coupled map lattice associated with the spring-block model of earthquakes is robust under a rather natural perturbation of its elastic constants. Although we have checked that for a perfect lattice $B(\alpha)$ is a smoothly decreasing function of α, we find that the presence of defects with $\alpha_d < \alpha$ results in a reduction of B that we tentatively associate with the nonlocal character of the update rules of the automaton.

Note added: We have become aware of a very recent and interesting work by P. Grassberger [13] where a more efficient algorithm for simulating this (and other similar) model in much larger lattices is introduced. The extension of the present work to these sizes could help to understand the relationship between avalanche scaling and the sources of spatial inhomogeneities, a subject raised in the Grassberger paper.

[1] P. Bak, C. Tang and K. Wiesenfeld, Phys. Rev. Lett. **59**, 381 (1987).
[2] T. Hwa and M. Kardar, Phys. Rev. Lett. **62**, 1813 (1989).
[3] H. J. S. Feder and J. Feder, Phys. Rev. Lett. **66**, 2669 (1991).
[4] Z. Olami, H. J. S. Feder, and K. Christensen, Phys. Rev. Lett. **68**, 1224 (1992).
[5] R. Burridge and L. Knopoff, Bull. Seismol. Soc. Am. **57**, 341 (1967).
[6] K. Christensen, Z. Olami, and P. Bak, Phys. Rev. Lett. **68**, 2417 (1992).
[7] J. Socolar, G. Grinstein, and C. Jayaprakash, Phys. Rev. E **47**, 2366 (1993). These authors argue that both the forest fire model and the present model (at least in the case of periodic boundary conditions) do not display true SOC behavior.
[8] K. Christensen and Z. Olami, Phys. Rev. A **46**, 1829 (1992).
[9] There are many other ways in which one could perturb this system. Any static perturbation can be characterized by describing the distribution of α values of the defects. For instance, one could use a zero mean, Gaussian (or uniform) distribution of width $\Delta\alpha$ on top of the initial value. We have chosen a perturbation with a *finite* mean value, keeping in mind the specific purpose of this work. Other physical motivations could suggest the use of other distributions.
[10] We have also collected data of the distribution of lifetimes of earthquakes, $D(t)$.
[11] B. Gutenberg and C. Richter, Ann. Geofys. **9**, 1 (1956). The original formulation of this law states that the rate of ocurrence of earthquakes of magnitude M greater than m is given by $\log_{10} N(M > m) = a - bm$ where a and b are constants characterizing the site. Both expressions are equivalent because it is usually assumed that the energy released increases exponentially with m.
[12] I. M. Jánosi and J. Kertész, Physica A **200**, 179 (1993).
[13] P. Grassberger, Phys. Rev. E **49**, 2436 (1994).